Draft version May 8, 2009
Preprint typeset using LaTeX style emulateapj v. 10/09/06

INTERACTIONS OF GALAXIES IN THE GALAXY CLUSTER ENVIRONMENT

Changbom Park and Ho Seong Hwang
School of Physics, Korea Institute for Advanced Study, Seoul 130-722, Korea
Draft version May 8, 2009

ABSTRACT

We study the dependence of galaxy properties on the clustercentric radius and the environment attributed to the nearest neighbor galaxy using the Sloan Digital Sky Survey (SDSS) galaxies associated with the Abell galaxy clusters. We find that there exists a characteristic scale where the properties of galaxies suddenly start to depend on the clustercentric radius at fixed neighbor environment. The characteristic scale is $1 \sim 3$ times the cluster virial radius depending on galaxy luminosity. Existence of the characteristic scale means that the local galaxy number density is not directly responsible for the morphology-density relation in clusters because the local density varies smoothly with the clustercentric radius and has no discontinuity in general. What is really working in clusters is the morphology-clustercentric radius-neighbor environment relation, where the neighbor environment means both neighbor morphology and the local mass density attributed to the neighbor. The morphology-density relation appears working only because of the statistical correlation between the nearest neighbor distance and the local galaxy number density. We find strong evidence that the hydrodynamic interactions with nearby early-type galaxies is the main drive to quenching star formation activity of late-type galaxies in clusters. The hot cluster gas seems to play at most a minor role down to one tenth of the cluster virial radius. We also find that the viable mechanisms which can account for the clustercentric radius dependence of the structural and internal kinematics parameters are harassment and interaction of galaxies with the cluster potential. The morphology transformation of the late-type galaxies in clusters seems to have taken place through both galaxy-galaxy hydrodynamic interactions and galaxy-cluster/galaxy-galaxy gravitational interactions.

Subject headings: galaxies: clusters: general – galaxies: evolution – galaxies: formation – galaxies: general

1. INTRODUCTION

In galaxy clusters the average morphology of galaxies changes with clustercentric radius or local density. The central region of clusters at the present epoch is dominated by early-type galaxies. This is known as the morphology-radius or morphology-density relation (hereafter MRR and MDR, respectively). Since the local density is on average a monotonically decreasing function of clustercentric radius, they appear to convey us the same information (Hubble & Humason 1931; Dressler 1980; Dressler et al. 1997; Treu et al. 2003; Smith et al. 2005; Postman et al. 2005; Weinmann et al. 2006). However, there is discussion about which one plays a critical role in determining the galaxy morphology between the clustercentric radius and the local density (Whitmore et al. 1993; Domínguez et al. 2001; Goto et al. 2003; Thomas & Katgert 2006). There is also a remaining issue what physical parameters of galaxies (morphology, color, star formation rate, or stellar mass) correlate fundamentally with the environment (e.g., Christlein & Zabludoff 2005; Quintero et al. 2006; Poggianti et al. 2008; Skibba et al. 2008).

A number of physical mechanisms have been proposed to explain this morphology-environment relation. It is suggested that tidal interactions between individual galaxies can change mass profile and transform disk galaxies into spheroidals (Byrd & Valtonen 1990). Frequency of galaxy-galaxy interaction depends strongly on the clustercentric radius, and thus galaxy interactions can result in the MRR or MDR. However, the duration of tidal interactions and thus the total tidal energy deposit are expected to be too small to change galaxy properties significantly for cluster galaxies that are moving at high speeds. Due to the fast orbital motions the frequency of galaxy mergers is also small in clusters. A series of frequent high-speed tidal interactions among cluster galaxies, called harassment, can produce impulsive heating and cause morphology transformation (Moore et al. 1996). Tidal interaction with the whole cluster potential well can also change the structure and activity of galaxies significantly (Moss & Whittle 2000; Gnedin 2003).

Existence of the hot X-ray emitted by intracluster gas makes the mechanisms relying on hydrodynamic processes appear attractive. Stripping of cold gas from infalling late-type galaxies by a ram pressure of the hot intracluster gas, was proposed to explain the increase of the early-type fraction toward the cluster center (Gunn & Gott 1972). Hot gas removal from infalling galaxies through hydrodynamic interactions with the intracluster medium can shut off gas supply and star formation activity (SFA) after the already existing cold gas is consumed. The interstellar medium of a galaxy traveling in the hot intracluster medium can be stripped from the disk due to a viscosity momentum transfer (Nulsen 1982) or evaporate as the temperature of the interstellar medium rises (Cowie & Songaila 1977). These hydrodynamic processes have a common drawback that they can turn spirals only to S0's and do not produce ellipticals. The major effect of the hydrodynamic processes is quenching the SFA by removing or ionizing the cold gas

Electronic address: cbp@kias.re.kr, hshwang@kias.re.kr

in the disk of late-type galaxies. The bulge-to-disk ratio is not expected to increase by these processes. Therefore, none of the mechanisms proposed so far is able to fully account for the MRR or MDR observed in clusters.

Recently, Park et al. (2008) and Park & Choi (2009) have found that galaxy properties like morphology and luminosity depend strongly on the distance and morphology of the nearest neighbor galaxy. This dependence was found even when the large-scale background density is fixed, and thus is completely different from the commonly known morphology-local density relation. Most importantly, the effects of the nearest neighbor change at the characteristic scale given by the virial radius of the neighbor galaxy. When a galaxy is located within the virial radius of its nearest neighbor, its morphology tends to be the same as that of the neighbor. But such tendency disappears when the separation is larger than the virial radius. This fact strongly suggests that galaxies interact hydrodynamically when the separation to their nearest neighbor is smaller than the virial radius of the neighbor, and that the effects of such interaction are significant enough to change their morphology and SFA.

Outside the virial radius galaxy morphology still depends on the distance to the nearest neighbor, but is suddenly independent of neighbor's morphology. The probability for a galaxy to be an early type monotonically decreases as the separation increases. This strongly supports the idea that the conformity in morphology of galaxy pairs is not primordial but an acquired one through interactions since there should be no reason for the break in morphology conformity to be at the current virial radius of the neighbor if it is initially given. Park et al. (2008) proposed that the mechanism responsible for this be tidal interactions causing both gravitational and hydrodynamic effects. Outside the virial radius the interactions are purely gravitational between the galaxy plus dark halo systems, but within the virial radius hydrodynamic (and radiative) effects must be involved as well.

A series of tidal interactions and mergers will keep the total cold gas contents in bright galaxies decreasing, producing more early-type galaxies as time passes (Park et al. 2008; Park & Choi 2009; Hwang & Park 2008). The speed of this process is an increasing function of the large-scale density. Namely, even though the direct physical processes affecting galaxy morphology are the gravitational and hydrodynamic interactions between neighboring galaxies, the large-scale background density appears to control galaxy morphology through its statistical correlation with the frequency and strength of galaxy-galaxy interactions. Given the knowledge that the MDR in most region of the universe (note that Park et al. did not resolve the cluster regions) is the result of galaxy-galaxy interactions, one can naturally suspect the MRR and MDR in clusters are also due to the interactions between individual galaxies. It is the purpose of this paper to explore this possibility.

2. OBSERVATIONAL DATA SET

2.1. *Sloan Digital Sky Survey Sample*

We use a spectroscopic sample of galaxies in the Sloan Digital Sky Survey (SDSS) Data Release 6 (DR6; Adelman-McCarthy et al. 2008). The survey produced five-band (*ugriz*) photometric data for 230 million objects over 8,400 deg^2, and optical spectroscopic data more than one million objects of galaxies, quasars, and stars over 6860 deg^2 (Gunn et al. 1998, 2006; Uomoto et al. 1999; Castander et al. 2001; Blanton et al. 2003; Fukugita et al. 1996; Lupton et al. 2002; Hogg et al. 2001; Smith et al. 2002; Ivezić et al. 2004; Tucker et al. 2006; Pier et al. 2003). Extensive description of SDSS data products is given by York et al. (2000) and Stoughton et al. (2002).

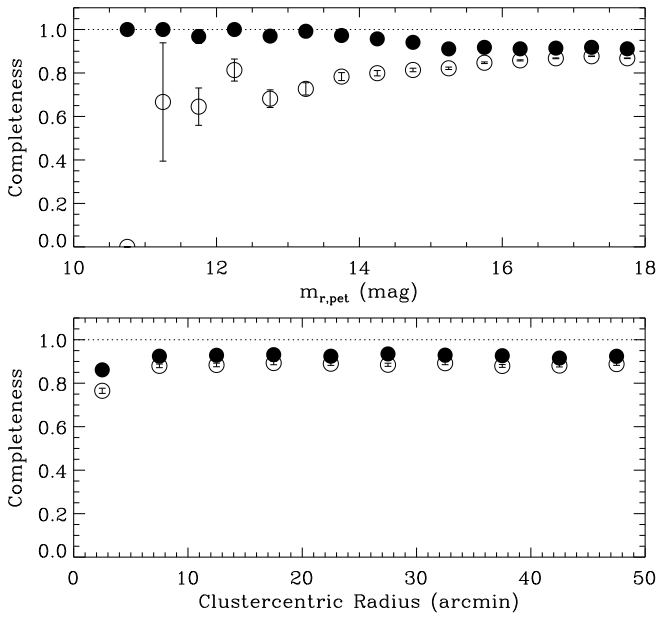

FIG. 1.— Completeness of the spectroscopic sample of cluster galaxies as a function of r-band magnitude (*upper panel*) and clustercentric radius (*lower panel*). Filled circles are the spectroscopic completeness of the data complemented by NED, while open circles show the completeness of the original SDSS spectroscopic sample.

The data is supplemented by several value-added galaxy catalogs (VAGCs) drawn from SDSS data. Photometric and structure parameters of galaxies are obtained from the SDSS pipeline (Stoughton et al. 2002). Complementary photometric parameters such as color gradient, concentration index, and Petrosian radius are taken from the DR4plus sample of Choi et al. (2007). The spectroscopic parameters are obtained from MPA/JHU and NYU VAGCs (Tremonti et al. 2004; Blanton et al. 2005).

Completeness of the spectroscopic data in SDSS is poor for bright galaxies with $m_r < 14.5$ because of the problems of saturation and cross-talk in the spectrograph, and for the galaxies located in high density regions such as galaxy clusters due to the fiber collision (two spectroscopic fibers cannot be placed closer than $55''$ on a given plate). Therefore, it is necessary to supplement the galaxy data to reduce the possible effects of the incompleteness problem. We search for the galaxies within ten times the virial radius of each galaxy cluster in the photometric catalog of the SDSS galaxies, and find their redshifts from the NASA Extragalactic Database (NED) to supplement our spectroscopic sample. Figure 1 shows the spectroscopic completeness of our galaxy sample as a function of apparent magnitude and of clustercentric distance. The open circles are the completeness of the

original SDSS sample, and the filled circles are that of our sample with additional redshifts. It shows that the spectroscopic completeness of our sample is higher than 85% at all magnitudes and clustercentric radii.

2.2. *Cluster Sample and Galaxy Membership in Clusters*

We used the Abell catalog of galaxy clusters (Abell et al. 1989) to identify cluster galaxies in our galaxy sample. Among the Abell clusters, we selected those that have known spectroscopic redshifts in the NED. We found 730 clusters located within the SDSS survey region. We adopted the position of cluster center in the NED, but replaced it with the X-ray determined position if it is available in the literature.

In order to determine the membership of galaxies in a cluster, we used the "shifting gapper" method of Fadda et al. (1996) that was used for the study of kinematics of galaxy clusters (Hwang & Lee 2007, 2008). In the radial velocity versus clustercentric distance space, the cluster member galaxies were selected by grouping galaxies with connection lengths of 950 km s^{-1} in the direction of the radial velocity and of 0.1 h^{-1}Mpc in the direction of the clustercentric radius R. If the boundary was not reached out to $R = 3.5h^{-1}$Mpc, we stopped the grouping at $R = 3.5h^{-1}$Mpc. We iterated the procedure until the number of cluster members converges. From this procedure we obtained 200 Abell clusters that have more than or equal to 10 member galaxies.

We computed a radius of $r_{200,\rm cl}$ (usually called the virial radius) for each cluster where the mean overdensity drops to 200 times the critical density of the universe $\rho_{\rm c}$, using the formula given by Carlberg et al. (1997):

$$r_{200,\rm cl} = \frac{3^{1/2}\sigma_{\rm cl}}{10H(z)}, \quad (1)$$

where $\sigma_{\rm cl}$ is a velocity dispersion of a cluster and the Hubble parameter at z is $H^2(z) = H_0^2[\Omega_m(1+z)^3 + \Omega_k(1+z)^2 + \Omega_\Lambda]$ (Peebles 1993). Ω_m, Ω_k, and Ω_Λ are the dimensionless density parameters. The velocity dispersion was computed for each cluster from the redshift distribution of the cluster member galaxies as described in Appendix.

In addition to the sample of cluster member galaxies obtained by the "shifting gapper" method above, we included the galaxies located at projected separations of $R_{max} < R < 10r_{200,\rm cl}$ to investigate the variation of galaxy properties over a wide range of clustercentric radius. R_{max} is the largest clustercentric distance of the cluster member galaxies determined above. These additional galaxies were constrained to have velocity difference relative to the cluster's systematic velocity less than $\Delta v = |v_{\rm gal} - v_{\rm sys}| = 1000$ km s^{-1}. The final sample consists of galaxies smoothly distributed from the cluster center to $R = 10r_{200,\rm cl}$ for each cluster. Figure 2 shows the radial velocities of galaxies around eight clusters in our sample as a function of clustercentric distance of galaxies.

We rejected the clusters that appeared to be interacting or merging, which was decided in the galaxy velocity versus clustercentric distance space. Dynamically young clusters having the brightest cluster galaxy (BCG) at large clustercentric distance ($R_{\rm BCG} > 0.18\,h^{-1}$ Mpc) were rejected too. We also eliminated the clusters for which survey coverages were not complete out to $10r_{200,\rm cl}$. We finally obtained a sample of 93 relaxed Abell clusters and 34,420 associated galaxies for our analysis.

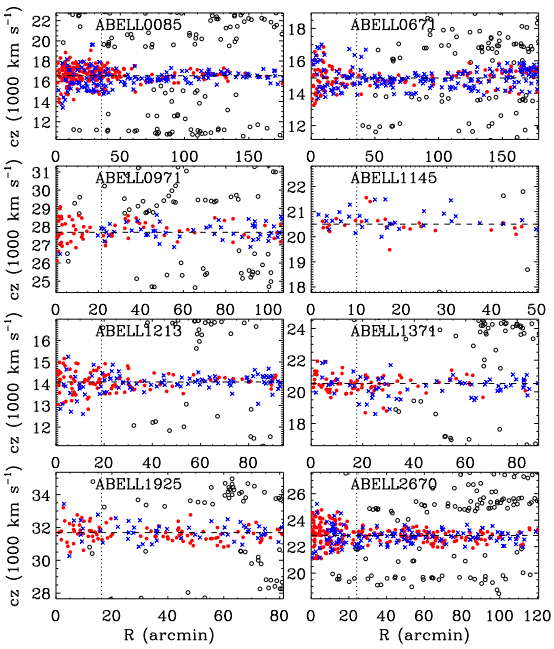

FIG. 2.— Radial velocity vs. clustercentric distance of galaxies. Filled circles and crosses indicate the early and late types, respectively, selected as galaxies associated with clusters, while open circles indicate the galaxies not selected as associated members. The horizontal dashed lines indicate the systemic velocity of the clusters determined in this study. The vertical dotted lines indicate the radius $r_{200,\rm cl}$ computed in this study.

2.3. *Physical Parameters of Galaxies*

The physical parameters of galaxies that we consider in this study are r-band absolute Petrosian magnitude (M_r), morphology, axis ratio, $u-r$ color, equivalent width of $H\alpha$ emission line, $g-i$ color gradient, concentration index ($c_{\rm in}$), internal velocity dispersion (σ), and Petrosian radius in i-band. Here we give a brief description of these parameters.

The r-band absolute magnitude M_r was computed using the formula,

$$M_r = m_r - 5\log[r(z)(1+z)] - 25 - K(z) - E(z), \quad (2)$$

where $r(z)$ is the comoving distance at redshift z in unit of h^{-1}Mpc, and the corresponding $5\log h$ term in M_r will be omitted in this paper. $K(z)$ is the K-correction, and $E(z)$ is the luminosity evolution correction. We adopt a flat ΛCDM cosmology with density parameters $\Omega_\Lambda = 0.73$ and $\Omega_m = 0.27$. The rest-frame absolute magnitudes of individual galaxies are computed in fixed bandpasses, shifted to $z = 0.1$, using Galactic reddening correction (Schlegel et al. 1998) and K-corrections as described by Blanton et al. (2003). The evolution correction given by Tegmark et al. (2004), $E(z) = 1.6(z-0.1)$, is also applied.

Figure 3 shows the r-band absolute magnitudes of the cluster galaxies against their redshifts. We define the volume-limited samples of galaxies using the redshift and absolute magnitude conditions as follows: C1 ($-17.0 \geq$

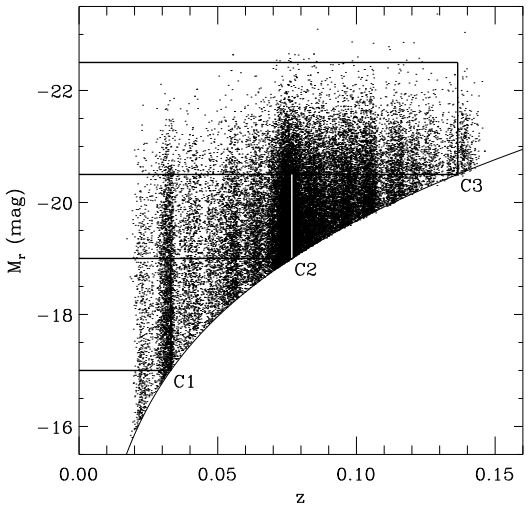

FIG. 3.— Sample definitions of our three volume-limited samples in the absolute magnitude vs. redshift space. The bottom curve corresponds to the apparent magnitude limit of $m_r = 17.77$.

$M_r > -19.0$ and $z \leq 0.0331$), C2 ($-19.0 \geq M_r > -20.5$ and $z \leq 0.0767$), and C3 ($-20.5 \geq M_r > -22.5$ and $z \leq 0.1365$). The apparent magnitude limit line ($m_r = 17.77$) shown in Figure 3 is obtained using the mean K-correction relation given by equation (2) of Choi et al. (2007).

Accurate morphology classification is critical in this work since the effects of interaction depend strongly on morphology of the target and neighbor galaxies. We first classify morphological types of galaxies included in the DR4plus sample of Choi et al. (2007) adopting the automated classification method given by Park & Choi (2005). Galaxies are divided into early (elliptical and lenticular) and late (spiral and irregular) morphological types based on their locations in the $u-r$ color versus $g-i$ color gradient space and also in the i-band concentration index space. The resulting morphological classification has completeness and reliability reaching 90%. The automatic classification scheme does not perform well when an early-type galaxy starts to overlap with another galaxy. This is because the scheme excludes galaxies with very low concentration from the early-type class and blended images often erroneously give low concentration. Since we are investigating the effects of close galaxy-galaxy and galaxy-cluster interactions on galaxy properties, this problem in the automatic classification has to be remedied. We perform an additional visual check of the color images of galaxies to correct misclassifications by the automated scheme. In this procedure we changed the types of the blended or merging galaxies, blue but elliptical-shaped galaxies, and dusty edge-on spirals. In addition, for the galaxies in DR6 that are not in the DR4plus sample, we visually classified their morphological types using the color images.

The $^{0.1}(u-r)$ color was computed using the extinction and K-corrected model magnitude. The superscript 0.1 means the rest-frame magnitude K-corrected to the redshift of 0.1, and will subsequently be dropped.

We adopt the values of $(g-i)$ color, concentration index ($c_{\rm in}$), and Petrosian radius $R_{\rm Pet}$ computed for the DR4plus sample of galaxies (Choi et al. 2007). The $(g-i)$ color gradient was defined by the color difference between the region with $R < 0.5R_{\rm Pet}$ and the annulus with $0.5R_{\rm Pet} < R < R_{\rm Pet}$, where $R_{\rm Pet}$ is the Petrosian radius estimated in i-band image. To account for the effect of flattening or inclination of galaxies, elliptical annuli were used to calculate the parameters. The (inverse) concentration index is defined by R_{50}/R_{90}, where R_{50} and R_{90} are semimajor axis lengths of ellipses containing 50% and 90% of the Petrosian flux in the i-band image, respectively.

The velocity dispersion value of the galaxy is adopted from NYU-VAGC (Blanton et al. 2005). The value of $H\alpha$ equivalent width is taken from MPA/JHU-VAGC (Tremonti et al. 2004), which is computed using the straight integration over the fixed bandpass from the continuum-subtracted emission line with the model of Bruzual & Charlot (2003).

In our analysis we often limit the late-type galaxy sample to galaxies with i-band isophotal axis ratio b/a greater than 0.6. This is to reduce the effects of internal extinction on our results. The absolute magnitude and color of late-type galaxies with $b/a < 0.6$ are very inaccurate (see Figs. 5 and 12 of Choi et al. 2007). Therefore, including them in the analysis may introduce a large dispersion in SF indicators such as luminosity, color, $H\alpha$ equivalent width, and color gradient.

2.4. *Nearest Neighbor Galaxy in Clusters*

To account for the effects of the nearest neighbor galaxy in cluster environment, we determine the distance and the morphology of the nearest neighbor galaxy.

We define the nearest neighbor galaxy of a target galaxy with absolute magnitude M_r as the one which is located closest to the galaxy on the sky and is brighter than $M_r + \Delta M_r$ among those in our cluster galaxy sample. We adopt $\Delta M_r = 0.5$. When we adopt galaxies fainter than the target galaxy by more than 0.5 mag as neighbors, our conclusions do not change but our statistics are worse since the number of target galaxies becomes smaller (see §3.1 for more discussion).

We do not use the velocity condition to determine the nearest neighbor galaxy because it is selected from the cluster galaxy sample to which the velocity condition is already applied. We obtain the nearest neighbor distance normalized by the virial radius of the nearest neighbor as follows. We first compute the small-scale density experienced by a target galaxy attributed to its neighbor,

$$\rho_n/\bar{\rho} = \gamma_n L_n/(4\pi r_p^3 \bar{\rho}/3), \quad (3)$$

where γ_n is the mass-to-light ratio of the neighbor galaxy, L_n is the r-band luminosity of the neighbor, r_p is the projected separation of the neighbor from the target galaxy, and $\bar{\rho}$ is the mean density of the universe. We assume that γ(early)=2γ(late) at the same r-band luminosity, and that γ is constant with galaxy luminosity for a given morphological type. The value of mean density of the universe, $\bar{\rho} = (0.0223 \pm 0.0005)(\gamma L)_{-20}(h^{-1}{\rm Mpc})^{-3}$, was adopted, where $(\gamma L)_{-20}$ is the mass of a late-type galaxy with $M_r = -20$ (Park et al. 2008).

Then, we define the virial radius of a neighbor galaxy as the projected radius where the mean mass density ρ_n within the sphere with radius of r_p is 200 times the critical density or 740 times the mean density of the universe,

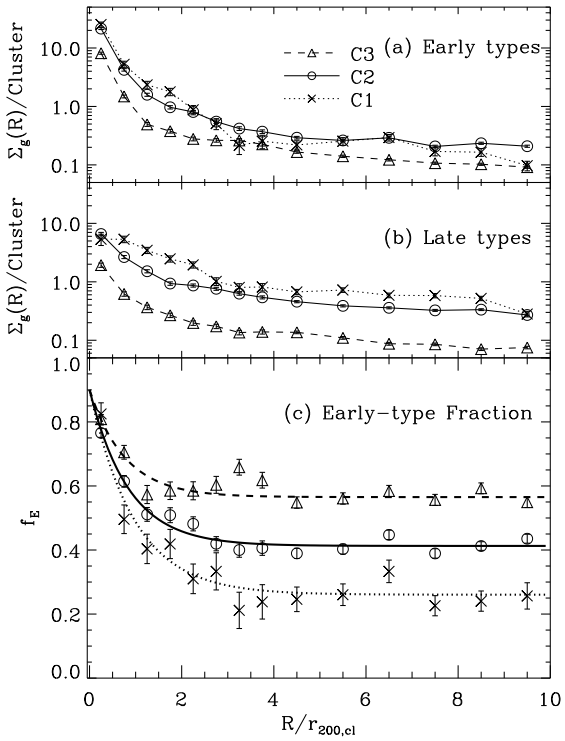

FIG. 4.— The surface number density of early-type (upper panel) and late-type (middle panel) galaxies in the Abell cluster regions, and the corresponding early-type fraction (bottom panel) as a function of the clustercentric radius normalized to the cluster virial radius. The lines in the bottom panel are the best-fitting functions.

namely,

$$r_{\rm vir} = (3\gamma L/4\pi/200\rho_c)^{1/3}. \quad (4)$$

Since we adopt $\Omega_m = 0.27$, $200\rho_c = 200\bar{\rho}/\Omega_m = 740\bar{\rho}$. This is almost equal to the virialized density $\rho_{\rm virial} = 18\pi^2/\Omega_m(H_0t_0)^2\bar{\rho} = 766\bar{\rho}$ in the case of our ΛCDM universe (Gott & Rees 1975). This is what Park et al. (2008) used to define the virial radius. According to our formula the virial radii of galaxies with $M_r = -19.5, -20.0$, and -20.5 are 260, 300, and 350 h^{-1} kpc for early types, and 210, 240, and 280 h^{-1} kpc for late types, respectively.

3. RESULTS

3.1. *Morphology-Environment Relation*

Figure 4 shows the surface number density of galaxies and the fraction of early-type galaxies as a function of projected clustercentric radius R normalized by the cluster virial radius $r_{200,\rm cl}$. They are shown for three luminosity ranges. The uncertainties of the fraction represent 68% (1σ) confidence intervals that are determined from the numerical bootstrap procedure.

It shows the well-known MRR or MDR of galaxies in clusters. In all three luminosity ranges the early-type fraction f_E is almost constant at large distances, and starts to increase inwards at the critical region with $R \approx 1 \sim 3r_{200,\rm cl}$, which corresponds to the cluster infall region. The transition radius seems depending on galaxy luminosity. For relatively brighter galaxies with $-20.5 \geq M_r > -22.5$ (the subsample C3) the transition occurs at $\sim 1.5r_{200,\rm cl}$, but for fainter galaxies with $-17.0 \geq M_r > -19.0$ (the subsample C1) it occurs at $\sim 3r_{200,\rm cl}$. The slope of increase is larger for less luminous galaxies at small R. Since we are not distinguishing between ellipticals and lenticulars, we can only see their sum is rising toward the cluster center. Fainter galaxies seem more vulnerable to the cluster influence. This can be considered as evidence for the direct interaction between clusters and infalling galaxies, thinking that less massive galaxies change their morphology at farther distances from clusters relative to massive ones. However, it can be also due to the mass segregation within clusters that massive cluster member galaxies hardly overshoot beyond the cluster virial radius while the less massive ones overshoot out to a few times the virial radius. Massive galaxies outside the virial radius are likely to be the infalling ones rather than bound cluster members.

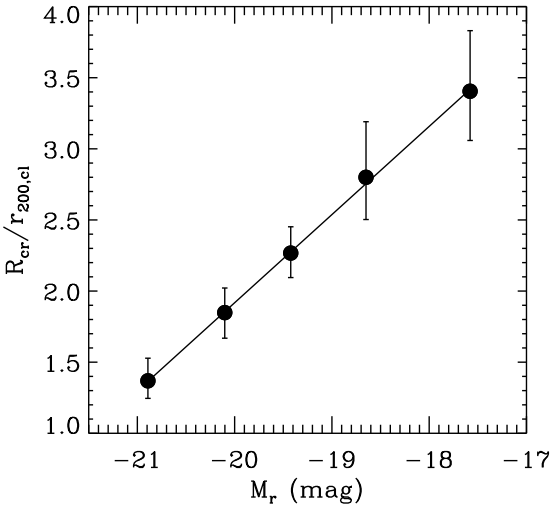

FIG. 5.— The characteristic clustercentric radius $R_{\rm cr}$ as a function of r-band absolute magnitude. $R_{\rm cr}$ is the scale where the early-type fraction f_E starts to rise significantly above the field value. Five luminosity subsamples are used: $-17 \geq M_r > -18, -18 \geq M_r > -19, -19 \geq M_r > -19.75, -19.75 \geq M_r > -20.5, -20.5 \geq M_r > -22.5$. The best-fit linear line is $R_{\rm cr}/r_{200,\rm cl} = (0.62 \pm 0.10)M_r + (14.32 \pm 1.95)$.

Figure 4 indicates that the early-type fraction is nearly the same near the cluster center regardless of galaxy luminosity. The central value of $f_E = 0.8 \sim 0.85$ actually means that the fraction is close to 1.0 at the cluster center if the projection effect is taken into account (Ann et al. 2008). At radii larger than about $4r_{200,\rm cl}$, f_E approaches the field fraction that depends on the luminosity range and becomes insensitive to the large-scale environment (Park et al. 2007).

To inspect this characteristic scale in more details we fit f_E as a function of $R/r_{200,\rm cl}$ using the function

$$f_E = (0.9 - f_0)\exp(-R/R_0) + f_0, \quad (5)$$

where R_0 is a free parameter and f_0 is an average value of f_E at $R/r_{200,\rm cl} > 4.0$. We define the characteristic radius $R_{\rm cr}$ as the scale where f_E becomes 10% larger than its field value at fixed luminosity. Figure 5 shows an almost linear relation between the characteristic radius and the absolute magnitude obtained from five luminosity subsets. The best-fit linear line is $R_{\rm cr}/r_{200,\rm cl} = (0.62 \pm 0.10)M_r + (14.32 \pm 1.95)$.

We now investigate the dependence of galaxy morphology on both clustercentric radius and nearest neighbor

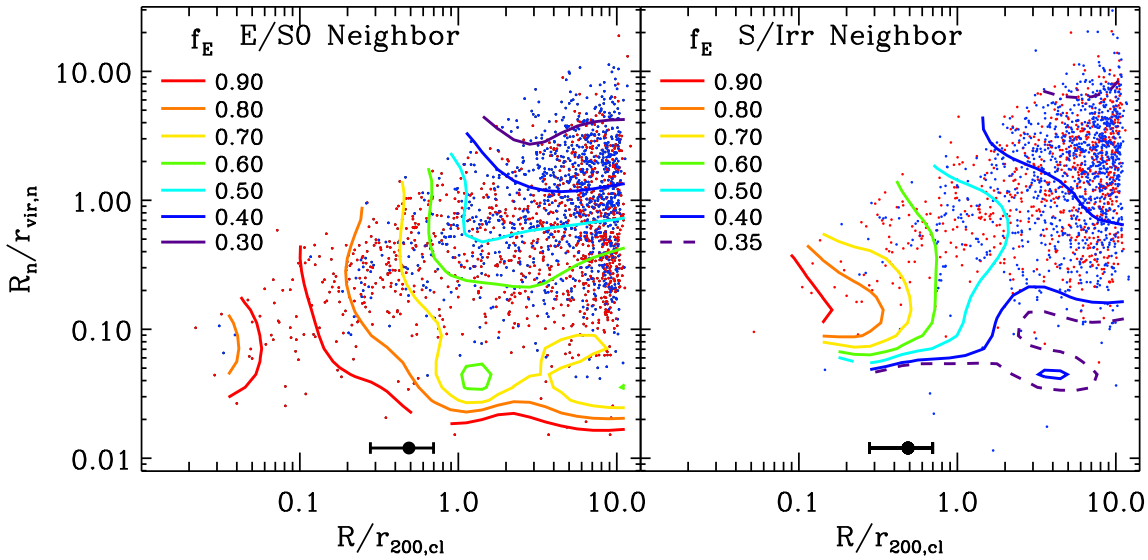

FIG. 6.— Morphology-environment relation when the nearest galaxy is (left) an early-type and (right) a late-type. Absolute magnitude of galaxies is fixed to a narrow range of $-19.5 \geq M_r > -20.0$. Contours show constant early-type galaxy fraction f_E. The points with error bars above the x-axes denote the average virial radius of the BCGs.

distance. We select a volume-limited sample of target galaxies associated with clusters whose absolute magnitudes are in a narrow range of $-19.5 \geq M_r > -20.0$ and redshifts are less than 0.0767. Their nearest neighbors are found among all galaxies with $M_r \leq -19.0$. Then $r_{\rm vir}$ of the nearest neighbors are calculated using their luminosity and morphology.

Dots in Figure 6 show the distribution of early-type (*red points*) and late-type (*blue points*) galaxies in the projected clustercentric radius R and projected nearest neighbor distance R_n space. A spline kernel is used to obtain the smooth distributions of the median f_E in each location of the two panels. Contours with different colors mark constant early-type fractions. The left panel of Figure 6 contains the target galaxies having early-type neighbors. It shows that at $R \gtrsim 2r_{200,\rm cl}$ all contours are nearly horizontal. This means that outside the cluster virial radius galaxy morphology is determined solely by the nearest neighbor distance and morphology. When the nearest neighbor is an early type, f_E monotonically increases as R_n decreases. But if the neighbor is a late type, it first increases, reaches a maximum at $R_n \sim r_{\rm vir,n}/3$, and then decreases as R_n decreases. The bifurcation occurs at $R_n \sim r_{\rm vir,n}$. This is the morphology-neighbor environment relation that was discovered by Park et al. (2008) in the general large-scale background density environment. It is interesting to see that the effects of the nearest neighbor's distance and morphology are the dominant factors of galaxy morphology transformation right down to the cluster infall regions.

The situation abruptly changes at the critical clustercentric radii of $R_{\rm cr} = 1 \sim 3r_{200,\rm cl}$. Within this radius contours are nearly vertical when $R_n \gtrsim 0.1r_{\rm vir,n}$, but are nearly horizontal when $R_n \lesssim 0.05r_{\rm vir,n}$. When $R_n \gtrsim 0.1r_{\rm vir,n}$, f_E monotonically increase as R decreases and depends almost entirely on R regardless of the morphological type of the nearest neighbor. Existence of this sudden transition near the cluster virial radius suggests that the morphology transformation of cluster galaxies is due to the interactions between galaxies and clusters. Both gravitational and hydrodynamic processes can produce the discontinuity in f_E. It may be the hot cluster gas confined within $\sim r_{200,\rm cl}$ or gravitational tidal force of cluster acting on galaxies trapped within the virial radius that causes the transformation. The monotonic increase of f_E at smaller R can arise by the increase of the effects of hot cluster gas whose pressure monotonically increases toward the cluster center and/or by interactions with the cluster potential for galaxies with smaller orbital radii that have the shorter crossing time.

On the other hand, Figure 6 clearly indicates that the clustercentric radius is not the only environmental parameter determining the galaxy morphology but the nearest neighbor does a critical role when the neighbor separation is less than about $0.05r_{\rm vir,n}$. The local galaxy number density, to which the MDR is often attributed, cannot be responsible for the increase of f_E inwards cluster because the density rises smoothly as R decreases and does not have a characteristic break at $R_{\rm cr}$ (see Fig. 4). After all, it is the morphology-clustercentric radius-neighbor environment relation instead of the simple MDR or MRR that determines the morphology of cluster galaxies. Here neighbor environment includes both neighbor distance and neighbor morphology.

We emphasize that we are not using the nearest neighbor distance as a measure of local galaxy number density. It is a measure of the influence of the nearest neighbor galaxy itself irrespectively of other galaxies. However, there exists statistical correlation between R_n and the local galaxy number density. If one uses a measure of local galaxy number density, one will still find some correlation of the measure with galaxy morphology within the cluster virial radius. But it is actually the galaxy-galaxy interaction that causes the correlation. This is because fixing R essentially fixes the local galaxy number density and in Figure 6 f_E still changes at a fixed R.

In the left panel of Figure 6 galaxies have early-type neighbors. It is expected that both cluster and neighbor galaxy impose morphology transformation toward early

type on galaxies through hydrodynamic or gravitational effects. Dominance of the role between the two depends on R and R_n. At $R \approx r_{200,\rm cl}$ the neighbor galaxy starts to give a major impact on galaxy morphology at the separations $R_n < 0.5r_{\rm vir,n} = 100 \sim 150h^{-1}$kpc (note the difference of f_E between the two panels). But at $R \approx 0.2r_{200,\rm cl}$ it happens at $R_n < 0.05r_{\rm vir,n} \approx 10 \sim 15h^{-1}$kpc. This seems reasonable since near the cluster center the tidal effects by the cluster potential are stronger, the cluster gas has higher pressure, and thus the cluster gives more direct impact on galaxy properties.

One can note from a comparison between two panels of Figure 6 that directions and levels of contours change completely depending on the morphology of the nearest neighbor galaxy at any clustercentric radius when the pair separation is small (i.e. $R_n \lesssim 0.1r_{\rm vir,n}$). The right panel shows that a cluster galaxy tends to become a late type when it has a late-type neighbor within the separation $R_n \approx 0.1r_{\rm vir,n}$ even when the pair is well within the cluster virial radius. For pairs with $R_n \approx 0.05r_{\rm vir,n}$ $f_E \approx 0.8$ at the clustercentric radius of $R = 0.5r_{200,\rm cl}$ when the neighbor is an early type. But f_E is as low as 0.35 for pairs with the same R_n located at the same R when the neighbor is a late type. It is a clear demonstration that the nearest neighbor has a dominant control over galaxy morphology transformation in clusters when the distance to the neighbor is less than about one tenth of the virial radius of the neighbor galaxy.

Figure 6 shows that there are not many such short separation pairs at a particular moment within the cluster virial radius and one might think that the majority of cluster galaxies are not affected by neighbors. However, it can be seen in Figure 6 that at $R \lesssim 0.5r_{200,\rm cl}$ the mean separation between galaxies becomes so small that the virialized regions associated with galaxies are all overlapping with one another (not that the upper edge of the galaxy distribution becomes smaller than $R_n/r_{\rm vir,n} = 1$ at $R/r_{200,\rm cl} \lesssim 0.5$ in Fig. 6). Suppose the RMS orbital velocity of galaxies within $r_{200,\rm cl}$ is $\langle v^2\rangle^{1/2}$. If $r_{200,\rm cl} = 1.5\ h^{-1}$ Mpc and $\langle v^2\rangle^{1/2} = 700$ km s^{-1}, the crossing time across $r_{200,\rm cl}$ is about 3×10^9 yrs. On the other hand, the RMS relative velocity between two random cluster galaxies is $\sqrt{2}\langle v^2\rangle^{1/2}$. If the virial radius of the galaxies is $r_{\rm vir} = 300\ h^{-1}$ kpc, their crossing time is 4×10^8 yrs, an order of magnitude shorter than the crossing time across the cluster. This means in this figure that the cluster galaxies at $R < r_{200,\rm cl}$ have migrated vertically (interaction with neighbor galaxies) many times during the time they make one travel horizontally (interaction with the cluster). In particular, when $R < 0.5r_{200,\rm cl}$, a galaxy starts to interact with another neighbor galaxy as it passes one neighbor galaxy because the virial radii of galaxies all overlap with one another there. Then the nearest neighbors may have left significant cumulative effects on morphology of cluster galaxies. The amount of the cumulative effects increases monotonically as the clustercentric radius decreases, which can produce the trend seen in Figure 6.

It is expected that the late-type galaxy sample has a higher fraction of interlopers in the cluster environment. The pairs involving late-type target or late-type neighbor are more likely to be false pairs, and more widely separated in real space. If this effect is corrected in Figure 6, the contours will be shifted upward. Furthermore, if the fraction of interlopers varies as a function of neighbor separation or clustercentric radius, the contours will be both shifted and stretched. However, the fact that there are discontinuities in f_E shown in Figure 6 (near the cluster virial radius $R \approx r_{200,\rm cl}$ and the galaxy merger scale $R_n \approx 0.05r_{\rm vir,n}$) and also the fact that these transitions occur at physically meaningful scales, cannot be explained if the fraction of interlopers is seriously high. This suggests that the morphology-environment relation shown by the contours in Figure 6 is not seriously affected by the interlopers.

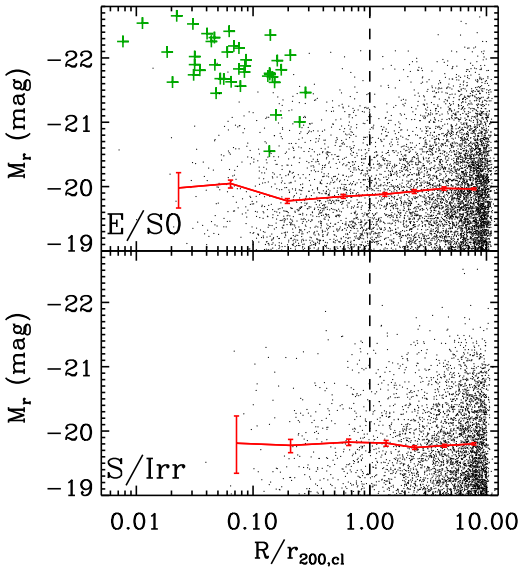

FIG. 7.— Absolute magnitude of galaxies brighter than $M_r = -19$ in the Abell cluster regions as a function of clustercentric radius. The upper panel shows the early types, and the lower panel shows the late types. Lines are the median magnitudes. Crosses are the BCGs, and they are not used in calculating the median values. Late types with axis ratio of $b/a < 0.6$ were eliminated. The vertical dashed lines indicate the cluster virial radius $r_{200,\rm cl}$.

Though we rejected the clusters that appear to be interacting or merging, there are some clusters ($\sim$15%) whose projected distance to the nearest cluster is less than $10r_{200,\rm cl}$ and relative velocity is less than 1000 km s^{-1}. Therefore, the galaxies associated with these clusters have been counted more than once in our analysis. For example, among 3874 galaxies used in Figure 6, 874 galaxies are those counted more than once. When we reject these galaxies, our results remain almost the same. In addition, our results do not depend sensitively on our definition of the nearest neighbor. For example, when we varied ΔM_r from 0.5 to 0.75, our results remain qualitatively the same (see also Park et al. 2008; Park & Choi 2009).

The mean virial radius of the BCGs, which is typically about $0.5r_{200,\rm cl}$, and its 1σ range are shown above the x-axes of Figure 6. We do not find any characteristic feature across the virial radius of the BCGs. This suggests that the BCGs are not directly participating in transforming the morphology of the cluster galaxies. When the positions of BCGs are used as the centers of clusters, the contours in Figure 6 are basically unchanged at $R \gtrsim 0.2r_{200,\rm cl}$. But the slight drop of f_E at $R < 0.1r_{200,\rm cl}$ seen for the E/S0 neighbor case, now disappears.

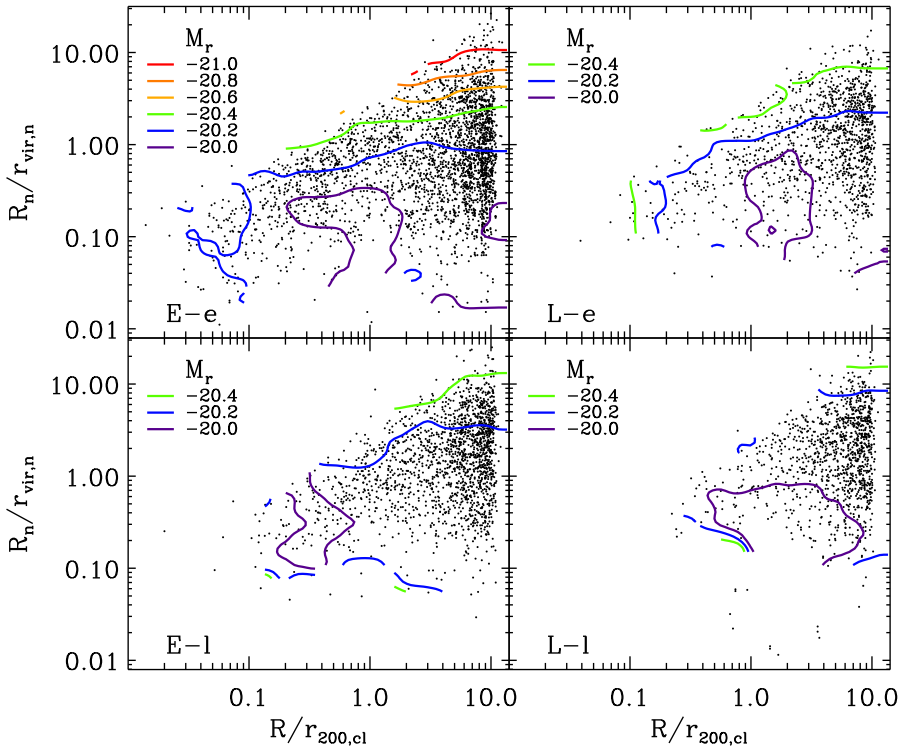

FIG. 8.— Median absolute magnitude contours in the projected pair separation $R_n/r_{\rm vir,n}$ vs. the clustercentric distance $R/r_{200,\rm cl}$ for the galaxies with $z \leq 0.0767$ and $M_r \leq -19.5$. Late types with axis ratio of b/a< 0.6 were eliminated. Four cases are given; the early-type target galaxies having an early-type neighbor (E-e), the early-type target galaxies having a late-type neighbor (E-l), the late-type target galaxies having an early-type neighbor (L-e), and the late-type target galaxies having a late-type neighbor (L-l).

3.2. *Luminosity-Environment Relation*

Figure 7 shows the r-band absolute magnitudes of the galaxies in a volume-limited sample with $z < 0.0767$ and $M_r < -19.0$. The lines with error bars are the median values as a function of R. The BCGs, marked as crosses, are not used in calculating the median values. Early-type galaxies become fainter as much as ~ 0.2 magnitude as R decreases from $10r_{200,\rm cl}$ to $0.2r_{200,\rm cl}$. The luminosity of early types rises again as R becomes smaller than about $0.2r_{200,\rm cl}$. But the increase of luminosity near the cluster center seems to depend on how much the BCGs are off-centered. Such a variation of the median luminosity is not detected for late types.

The dependence of luminosity on the environment can be better understood in the two dimensional study. Contours in Figure 8 delineate the constant median M_r locations in the two-dimensional environmental parameter space of R and R_n. Four panels distinguish among four different combinations of target and neighbor morphology. At each location of the R-R_n space the median value of M_r is found using the galaxies included within a spline kernel with a fixed size. The BCGs are not included in the smoothing.

It can be clearly seen that galaxies with larger R_n are brighter when R is greater than about $0.2r_{200,\rm cl}$. Namely, the bright galaxies are more isolated from their influential neighbors than the relatively faint galaxies are. In the region far outside the cluster virial radius the absolute magnitude of galaxies is nearly constant in R (i.e. the contours are nearly horizontal). Luminosity of galaxies with $R_n \gtrsim r_{\rm vir,n}$ depends very sensitively on R_n. But galaxies with $R_n < r_{\rm vir,n}$ show little dependence of M_r on R or R_n. The same phenomenon has been found by Park et al. (2008) for galaxy pairs in the general background density regions.

The reason that galaxies are brighter when they are located outside the nearest neighbor's virial radius was interpreted by Park et al. as due to luminosity transformation through mergers. After a galaxy merges with its closest neighbor, the second nearest neighbor will become the new nearest neighbor of the merger product. Since the merger product is typically located at a separation from the originally second nearest neighbor larger than the virial radius of the neighbor, a recently merged galaxy will appear in general at the upper edge of the galaxy distribution in Figure 8. As one moves toward the cluster center, the average galaxy number density increases and the mean distance between galaxies decreases. Correspondingly, the distance to the new nearest neighbor of a recently merged galaxy also decreases statistically for decreasing clustercentric radius, and the location of the recent merger products follows the upper edge of the galaxy distribution in Figure 8.

The upper left panel of Figure 8, showing the early-type target galaxies having early-type neighbors (the E-e case), shows that the maximum luminosity a galaxy can attain slowly decreases as R decreases until R becomes about $0.2r_{200,\rm cl}$. The median M_r of the most separated galaxies is about -21.3 at $R \approx 10r_{200,\rm cl}$, but decreases to about -20.0 at $R \approx 0.2r_{200,\rm cl}$, a more than one magnitude drop. This can be explained if the luminosity transformation process by galaxy-galaxy mergers becomes less efficient as R decreases. This is reasonable because the relative velocity between neighboring galax-

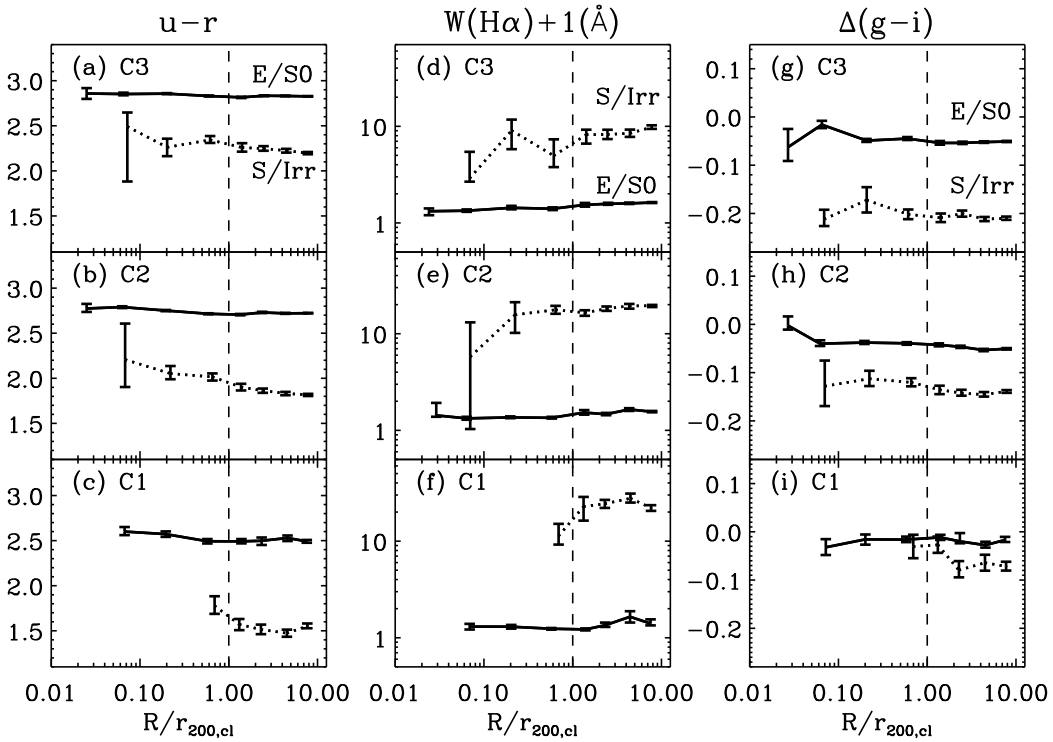

FIG. 9.— Dependence of star formation activity parameters of our target galaxies in the samples of C1, C2, and C3 on the clustercentric distance: (left) $u-r$, (middle) W(Hα)+1($\AA$), and (right) $\Delta(g-i)$. Median curves are drawn for the cases of early types (solid line) and of late types (dotted line). Late types with axis ratio of $b/a < 0.6$ were eliminated.

ies will be higher and the chance for a pair to merge will decrease toward the cluster center.

A similar R-dependent trend in luminosity is also seen for late-type galaxies as shown in the right panels of Figure 8 even though the trend is much weaker. Luminosity of late-type galaxies is on average lower than that of early types. Interestingly, the late-type galaxies having an early-type neighbor (the L-e galaxies) are slightly brighter than the early-type galaxies at $R \lesssim 0.1r_{200,\rm cl}$. It could be that, as R decreases, faint late types are transformed to early types and only relatively bright late types survive near the cluster center.

Figure 8 also shows that galaxies located near $R = r_{200,\rm cl}$ and having a close neighbor are on average the faintest. Namely, even though the most isolated galaxies become faintest at $R \approx 0.2r_{200,\rm cl}$, those with a close neighbor ($R_n \approx 0.1r_{\rm vir,n}$) become faintest at $R \approx 1.0r_{200,\rm cl}$.

3.3. *Star Formation Activity Parameters*

The left column of Figure 9 shows the $u-r$ color of galaxies divided into two morphology and three magnitude bins as a function of R. It can be seen that the galaxy color becomes redder as R decreases for both early and late types. This clustercentric radius dependence of color is stronger for relatively fainter galaxies (i.e. the C1 sample). In the case of the galaxies in C1 the dependence seems to occur at $\sim 3r_{200,\rm cl}$.

Dots in Figure 10 are the intermediate luminosity galaxies with $-19.5 \geq M_r > -20.5$ in the two-dimensional environmental parameter space. Color of early-type galaxies is nearly constant everywhere. There is a slight tendency that early-type galaxies become redder as they approach an early-type neighbor.

The constant color contours of late-type galaxies are nearly horizontal at $R > R_{\rm cr} = 1 \sim 3r_{200,\rm cl}$, which means galaxy color is independent of R and depends only on the neighbor separation R_n. Inside the critical radius $R_{\rm cr}$ the color of late-type galaxies still depends mainly on neighbor separation and morphology. This is evidence that hydrodynamic interactions between individual galaxies are effective even within the virialized region of clusters. In the case of the L-l galaxies there is clustercentric radius dependence of color when $R_n \gtrsim r_{\rm vir,n}/3$. It is likely that this is because the neighbors other than the nearest one tend to be early types as the system moves toward the cluster center. If the cluster hot gas had a direct impact on late-type galaxies' color, both L-e and L-l galaxies would show a similar color dependence on R.

The equivalent width of the hydrogen $H\alpha$ line is a measure of SFA. Figure 9 shows the median $W(H\alpha)$ as a function of R for six different cases distinguished by morphology and luminosity of target galaxies. The SFA of late-type galaxies decreases as R decreases. The dependence again seems to start at $\sim 3r_{200,\rm cl}$ for the galaxies in the C1 sample. It is important to note that both $u-r$ color and $W(H\alpha)$ show only mild dependence on the clustercentric radius R, and it is actually the neighboring galaxies that mainly determine the color and SFA of galaxies within clusters as we can see in Figure 10.

The second column of Figure 10 shows $W(H\alpha)$ in two-dimensional environmental parameter space. One can notice that the constant $W(H\alpha)$ contours look very similar to those of $u-r$ color. Namely, the SFA of the L-e galaxies is mainly controlled by the neighbor galaxies. On the other hand, the SFA of L-l galaxies shows dependence on R when the nearest neighbor separation is not too small ($R_n \gtrsim 0.3r_{\rm vir,n}$). This is again probably be-

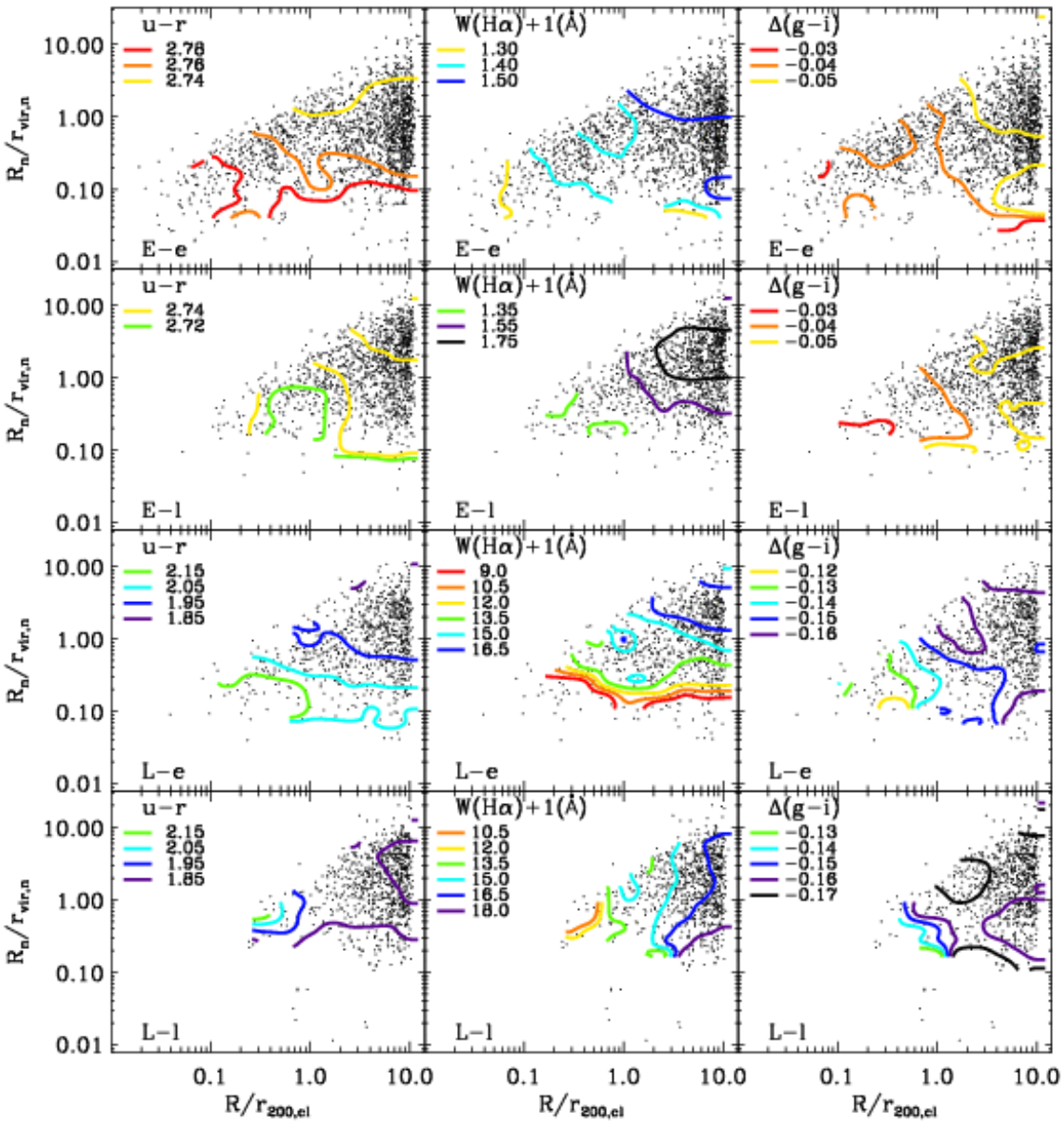

FIG. 10.— Dependence of $u-r$ color, equivalent width of the $H\alpha$ line, $g-i$ color gradient of galaxies with $-19.5 \geq M_r > -20.5$ on the pair separation R_n and the clustercentric distance R. In each column, galaxies are divided into four cases, the E-e, E-l, L-e, and L-l galaxies. Dots are galaxies belonging to each subset. At each location of the $R_n/r_{\rm vir,n}$-$R/r_{\rm 200,cl}$ space the median value of the physical parameter is found from those of galaxies within a certain distance from the location. Curves are the constant-parameter contours. Late types with axis ratio of $b/a < 0.6$ were eliminated.

cause the neighbors other than the nearest one tend to be early types as R decreases. The two cases demonstrate that the SFA of the late-type cluster galaxies changes differently depending on the morphology of the neighbor galaxy even well inside the cluster virial radius. If the hot cluster gas could directly quench the SFA of late-type galaxies, both L-l and L-e galaxies would show the same R-dependence of SFA regardless of the morphology of the nearest neighbor. Since this is not the case, one can conclude that it is after all the galaxy-galaxy hydrodynamic interaction that gives the biggest impacts on the color and SFA of cluster galaxies and that, contrary to intuition, the hot cluster gas is not the main actor quenching the star formation in late-type cluster galaxies at least down to $R \approx 0.1 r_{\rm 200,cl}$. We have repeated our analyses using the fainter galaxies with $-17.5 \geq M_r > -19.0$, and arrived at the same conclusion. In the case of early-type galaxies the $W(H\alpha)$ parameter is very small and hardly changes.

Figure 9 shows that the color gradient of galaxies depends only weakly on R. In all cases the central region of galaxies becomes slightly bluer relative to the outskirts as R decreases. The dependence is stronger for fainter galaxies.

In the right column of Figure 10 contours represent the distribution of the median $\Delta(g-i)$ at each location of the R-R_n space. Unlike the $u-r$ color and $W(H\alpha)$, the color gradient $\Delta(g-i)$ of late-type galaxies depends on both R and R_n inside $r_{\rm 200,cl}$ as can be seen from the slant contours. We interpret this phenomenon as a result of galaxy-galaxy interaction. When a late-type galaxy approaches a neighbor closer than the virial radius of the

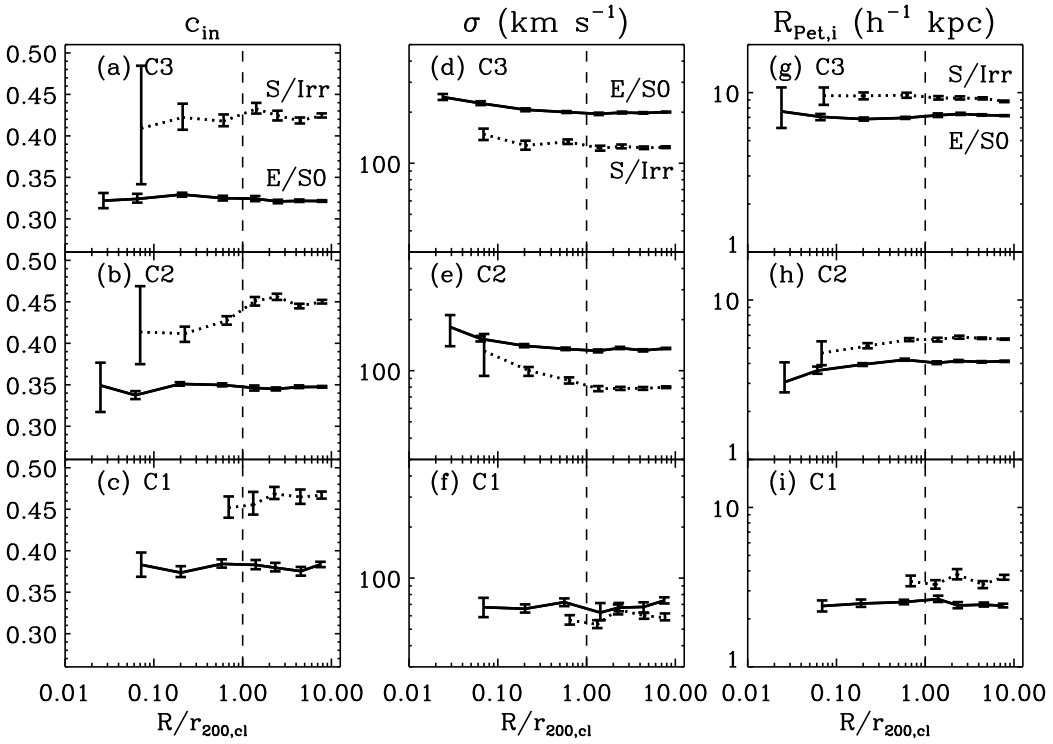

FIG. 11.— Same as Fig. 9, but for (left) $c_{\rm in}$, (middle) σ (km s^{-1}), and (right) $\rm R_{Pet,i}$ (h^{-1} kpc). Late-types with axis ratio of $b/a < 0.6$ were included.

neighbor, its color gradient always increases (center becomes relatively bluer) regardless of neighbor's morphology as shown by Park & Choi (2009, see Figs. 6 and 7). The color gradient of a late-type galaxy can increase as it moves toward the cluster center because it becomes more likely to be affected by neighbor galaxies. Since there is no neighbor morphology dependence of $\Delta(g-i)$ when a late type approaches a neighbor, the $\Delta(g-i)$ contours are quite similar for L-e and L-l galaxies. It is also possible that the center of late-type cluster galaxies becomes bluer at smaller R because of the tidal effects of the cluster potential (Merritt 1984).

3.4. *Structure Parameters*

The left column of Figure 11 shows that concentration of intermediate and low luminosity late-type galaxies increases (c_{in} decreases) as R decreases below $R_{\rm cr}$. But concentration of early types and high luminosity late types is nearly independent of R. As argued by Park & Choi (2009), this can be attributed to less compact internal structure of late types which are more vulnerable to tidal effects than early types.

The first column of Figure 12 shows the median c_{in} contours for the intermediate luminosity galaxies with $-19.5 \geq M_r > -20.5$. Again c_{in} of early types hardly changes as R or R_n vary. On the other hand, c_{in} of late types starts to decrease (galaxies become compacter) at $R \lesssim R_{\rm cr} = 1 \sim 3r_{200,\rm cl}$. It is interesting to see that the structural parameter c_{in} shows an abrupt change at the characteristic scale. A similar phenomenon can be found also for the central velocity dispersion.

The fact that the R-dependence of c_{in} exists only when $R \lesssim R_{\rm cr}$, gives an important clue for understanding the structural evolution of cluster galaxies. The local galaxy number density cannot be the reason for the discontinuous R-dependence of c_{in} because the local density is a smooth function of R. The discontinuity can appear due to repeated gravitational interactions of cluster member galaxies with cluster potential or with other galaxies as they make trapped orbital motions within the cluster virial radius. It might also seem possible to explain the discontinuity by the hydrodynamic effects of hot cluster gas. For example, the cold gas in the outer part of late-type galaxies can evaporate or be stripped when they fall into the hot cluster gas clump or encounter the hot halo gas of their neighbor galaxies. Then their outer part will become redder and dimmer. This may cause the color $u-r$ and color gradient $\Delta(g-i)$ increase and inverse concentration index c_{in} decreases as R or R_n decreases. However, it is difficult to explain why the central stellar velocity dispersion of late types should also increase shown in the second column of Figure 12 by quenching the SFA in the outer part.

Figure 11 (panels d, e, and f) shows that the central velocity dispersion of galaxies in general increases as R decreases except for low luminosity galaxies. The trend is clear for intermediate luminosity galaxies, in particular.

The second column of Figure 12 shows constant σ contours of intermediate luminosity ($-19.5 \geq M_r > -20.5$) galaxies divided into four different target-neighbor morphology cases. The central stellar velocity dispersion σ shows a characteristic behavior that it depends only on R_n at $R \gtrsim R_{\rm cr}$ but starts to depend only on R when $R \lesssim R_{\rm cr}$. Would the increase of σ within the cluster virial radius be due to the tidal interaction of galaxies with other galaxies or with the cluster potential? One can find a clue from Figure 11 which shows that the R-dependence of c_{in} and σ is largest for intermediate luminosity galaxies. This may be because the intermediate luminosity galaxies have suffered from the interac-

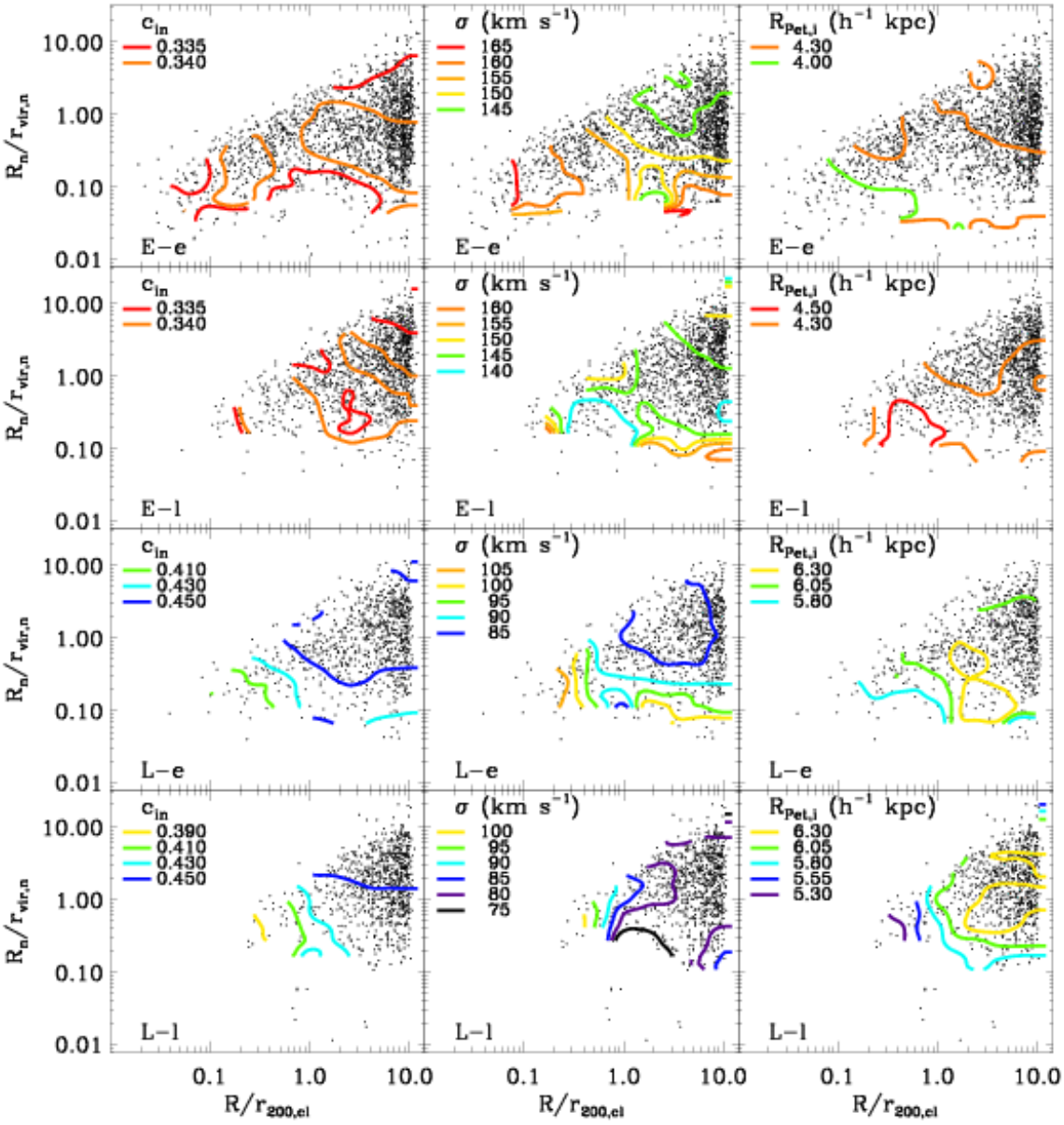

FIG. 12.— Same as Fig. 10, but for (left) $c_{\rm in}$, (middle) σ (km s^{-1}), and (right) $\rm R_{Pet,i}$ (h^{-1} kpc). Late-types with axis ratio of $b/a < 0.6$ were included.

tion with cluster potential more strongly than brighter or fainter ones. Even though galaxy-galaxy encounters in general increase σ of late-type galaxies (see L-e cases at $R > r_{200,\rm cl}$ and Fig. 8 of Park & Choi 2009), it is not true at $R < r_{200,\rm cl}$ as can be seen in Figure 12. The very bright massive galaxies at $0.1 \lesssim R/r_{200,\rm cl} \lesssim 1.0$ may be the galaxies falling into the cluster for the first time, and those which fell in long time ago are now sitting near the cluster center. In both cases the effects of the cluster potential will be relatively small. On the other hand, the small faint galaxies are likely to have large orbital radii, and can cross the cluster much fewer times than the massive ones. This is supported by the fact that $R_{\rm cr}$ is larger for fainter galaxies (see Fig. 5 for example). Therefore, it is expected that the intermediate luminosity galaxies are most susceptible to change in structure and kinematics through interactions with the cluster potential.

Our study of c_{in} and σ of cluster galaxies makes it clear that late-type galaxies become more centrally concentrated and have higher central velocity dispersion as they approach the cluster center. Our results suggest that late-type galaxies become earlier in SFA through hydrodynamic interactions between galaxies and also in morphology and kinematics through tidal interactions as they approach the cluster center. Paucity of late-type galaxies near cluster center is a result of combined effects of gravitational and hydrodynamic interaction with the cluster and the nearest neighbor galaxies.

We use the Petrosian radius in the i-band image as a measure of galaxy size. Figure 11 (panels g, h, and i) shows that the intermediate luminosity galaxies show very slight decrease of $R_{\rm Pet}$ as R decrease. The third column of Figure 12 shows again that there is a weak clustercentric radius dependence of $R_{\rm Pet}$ at $R \lesssim R_{\rm cr}$ for late-type galaxies. The decrease of $R_{\rm Pet}$ does not seem to be due to the blending of galaxy images in high density

regions like clusters because it suddenly occurs at the physically meaningful scale ($R_{\rm cr}$). The degree of blending of galaxy images should be a smooth function of R.

The size of late-type galaxies does not change significantly by interactions with other galaxies as shown in Figure 8 of Park et al. (2008). Therefore, the decrease of $R_{\rm Pet}$ of late types at $R < R_{\rm cr}$ shown in Figures 11 and 12 should be attributed to the cluster. Late-type galaxies can appear smaller when their outer part becomes dimmer as they orbit within a cluster and get quenched in star formation in disks.

4. DISCUSSION

Many mechanisms have been proposed to explain the MRR or MDR in clusters. They are divided into two categories : mechanisms relying on gravitational and hydrodynamic processes (see Boselli & Gavazzi 2006 for a review). The mechanisms based on gravitational interactions include galaxy-galaxy tidal interaction, galaxy-cluster potential tidal interaction, and interaction with the general tidal background (harassment). Those based on hydrodynamic interactions comprise ram pressure stripping, viscous stripping, or thermal evaporation of cold gas of late-type galaxies by hot cluster gas, and removal of hot halo gas reservoir causing stopping of gas supply and quenching of star formation (strangulation). We will examine each of these mechanisms against our findings.

1. Galaxy-galaxy tidal interaction

Tidal interaction between galaxies can be efficient at removing or consuming the cold gas in galaxies, and tend to transform late types into early types (Spitzer & Baade 1951; Richstone 1976; Farouki & Shapiro 1981; Icke 1985; Merritt 1983). However, this mechanism is usually excluded as a process responsible for the MRR or MDR because the orbital velocity of cluster galaxies are very high and the tidal energy deposit during the short encounters is too small to significantly affect galaxy structure (Merritt 1984; Byrd & Valtonen 1990).

At $R > R_{\rm cr}$, the structural parameter of late-type galaxies depend only on the environment determined by the neighbor galaxies. But $R < R_{\rm cr}$ they strongly depend on R, but only weakly or negligibly on R_n (see Fig. 12). This tells that the galaxy-galaxy tidal interactions do not instantly change the structure of cluster member galaxies much. The parameters c_{in} and $R_{\rm Pet}$ do show a weak dependence on R_n for L-e galaxies within $R = R_{\rm cr}$. But this may have also been resulted by hydrodynamic interactions with their early-type neighbor. Even though we exclude the significance of the tidal effects of galaxy-galaxy interactions on the internal structure and kinematics of cluster galaxies, it should be emphasized that the hydrodynamic effects of galaxy-galaxy interactions can give significant impacts on their SFA.

2. Galaxy-cluster potential interaction

Individual galaxies can suffer from the tidal force of the overall cluster mass (Merritt 1984; Miller 1986; Byrd & Valtonen 1990; Moss & Whittle 2000; Gnedin 2003). This mechanism is usually excluded in explaining the MRR or MDR because the time scale required for morphology transformation, being several cluster crossing time, is rather too long. The tidal force will be stronger toward the cluster center, and the strong dependence of c_{in} and σ on R within $R = R_{\rm cr}$ can easily explained by this mechanism. The internal structure of the intermediate mass galaxies, in particular, seems to have been significantly affected by this mechanism. But the tidal interaction with cluster potential may not be sufficient for morphology transformation of the very bright or faint cluster galaxies.

3. Harassment

Galaxies can be also perturbed by the tidal force background from numerous distant encounters with other cluster members (Moore et al. 1996, 1998, 1999). Even though individual encounters are too short for the tidal force to activate structural changes, galaxy structure may significantly change through such numerous weak encounters. The sudden transition of the structure parameters can be explained by repeated passage of member galaxies within the cluster. So both interaction with cluster potential and harassment may account for the R-dependence of morphology and structure parameters of intermediate mass galaxies, in particular, whose cluster crossing time is reasonably short but the path length is still long.

4. Galaxy-galaxy hydrodynamic interaction

The effects of hydrodynamic interaction between galaxies on cluster galaxy properties have been found important in this work. The galaxy-galaxy interaction turns out to be the major mechanism for quenching SFA of late-type galaxies within clusters. As can be seen in the scatter plot of galaxies in the R-R_n plane, distance to the neighbors monotonically decreases as R decreases and galaxies become always located within neighbor galaxy's virial radius when $R \lesssim R_{200,\rm cl}/3$. In this situation galaxies are constantly undergoing hydrodynamic effects and mass exchange with neighbors. We argued above that the vertical contours for c_{in} and σ can be explained by the gravitational tidal force from cluster itself. However, the nearly horizontal contours for the $u-r$ and $W(H\alpha)$ parameters can be only explained by hydrodynamic effects of neighbor galaxies. It should be emphasized that the high-speed orbital motion of cluster galaxies weakens the importance of galaxy-galaxy tidal interactions, but can make the galaxy-galaxy hydrodynamic interaction very important.

It was also found that bright galaxies are more isolated from influential neighbors than relatively fainter ones in clusters, which has been interpreted as due to merger-driven luminosity transformation. The fact that early-type galaxies show such trend more strongly is consistent with this interpretation. Relative paucity of bright galaxies near cluster center (except for the BCGs) seems to indicate that the frequency of galaxy merger decreases as the clustercentric radius decreases.

5. Ram Pressure Stripping

Many rich clusters like the Abell clusters we are analyzing, are holding hot X-ray emitting gas. A late-type galaxy falling into such a hot gas tank can strip off its cold gas and terminate SFA (Gunn & Gott 1972; Quilis et al. 2000). The hot gas is trapped roughly within the virial radius of the cluster. Therefore, any mechanism relying on hydrodynamic interaction with the hot cluster gas will have a characteristic scale of onset of cluster influence near the cluster virial radius.

A major problem with the ram pressure stripping and other hydrodynamic processes in accounting for the morphology segregation, is that these mechanisms can only

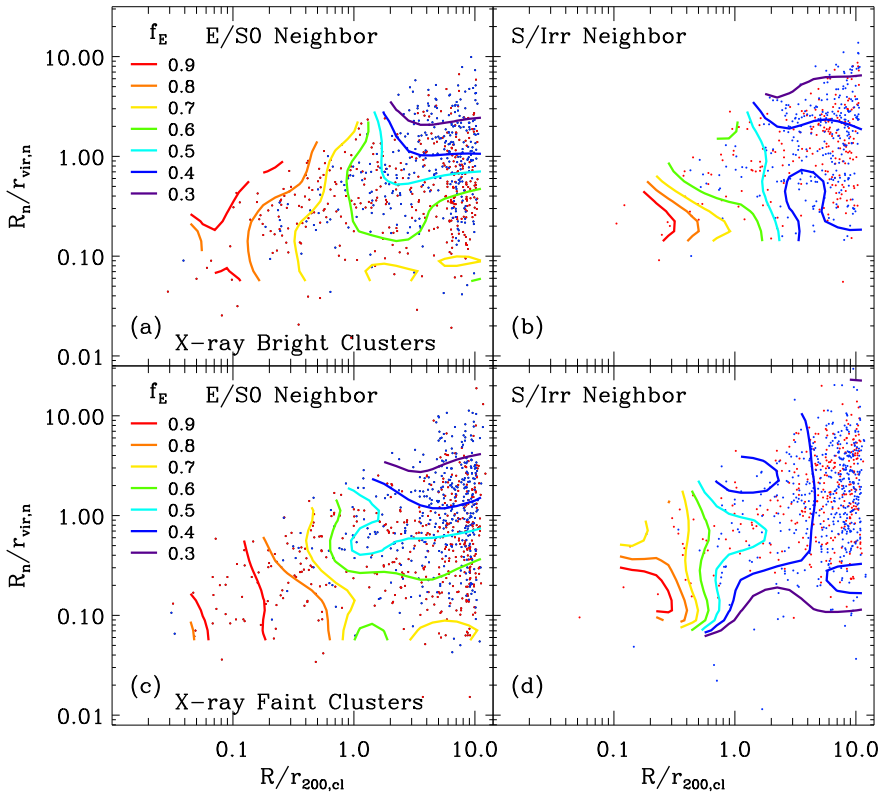

FIG. 13.— Same as Fig. 6, but for (a and b) X-ray bright clusters ($L_X \geq 2 \times 10^{44}$ erg s^{-1}) and (c and d) X-ray faint clusters ($0.6 \times 10^{44} \leq L_X \leq 2 \times 10^{44}$ erg s^{-1}). X-ray luminosities are from Böhringer et al. (2000, 2004).

reduce the SFA and cannot change galaxy structure while the observations require the fraction of bulge-dominated galaxies to increase significantly as the clustercentric radius decreases. Therefore, even though this mechanism can explain the radial variation of the fraction of galaxies that are red and inactive, it can not explain the radial variation of concentration or central velocity dispersion. It is also pointed out that only loosely bound thin clouds can be swept out of the galaxy and molecular clouds are mostly unaffected by this interaction (Quilis et al. 2000). Furthermore, we have shown in Figure 10 that it is actually the galaxy-galaxy interaction that mainly controls the color and SFA of the cluster late-type galaxies rather than the hot cluster gas.

6. Viscous stripping / Thermal evaporation

The cold gas in a late-type galaxy moving through the hot intracluster gas can be stripped off by momentum transfer between the cold disk gas and hot cluster gas (Nulsen 1982), or be evaporated by the thermal conduction (Cowie & Songaila 1977). These mechanisms can be activated when a galaxy fall into the hot cluster gas pool, and can give rise to a characteristic feature in the radial variation of galaxy SFA as observed in this work. However, they share the same problem the ram-pressure stripping mechanism has in that they can not modify galaxy structure.

Furthermore, the hot cluster gas cannot explain the environmental dependence of color and SFA of late-type galaxies either. If the hot cluster gas predominantly controls the color and SFA of cluster late types, the contours in Figure 10 should be vertical independently of R_n, which is not true.

7. Strangulation

According to the current understanding of galaxy evolution, spiral galaxies maintain SFA by accreting gas from their hot gas reservoir. It has been proposed that a spiral galaxy fell into the hot intracluster gas can lose its hot halo gas and stop supplying gas into its disk (Larson et al. 1980; Bekki et al. 2002). Then the galaxy just consume its already existing cold gas to form stars, and the SFA halts after some time when all cold gas is consumed. Compared to the ram pressure stripping, this mechanism will quench the SFA in late-type galaxies in a delayed action. As being a pure hydrodynamic process, it also has the problem that the structural parameters of galaxies can not be changed. This mechanism also predicts the contours to be vertical (dominance of cluster influence) for the early-type fraction, color, and SFA parameters in Figures 6 and 10, which is not supported by observations.

To inspect galaxy properties for their dependence on hot cluster gas in more details, we studied the early-type fraction in the R_n-R space separately for X-ray bright ($L_x \geq 2 \times 10^{44}$ erg s^{-1}) and faint ($0.6 \times 10^{44} \leq L_x \leq 2 \times 10^{44}$ erg s^{-1}) Abell clusters. Figure 13 shows that the magnitude of f_E is not particularly higher for X-ray bright clusters. This can be another evidence against the idea that the hot intracluster gas plays the main role in morphology transformation of late-type galaxies in massive clusters.

To summarize, the interaction responsible for the MRR/MDR in clusters can be either galaxy-galaxy or galaxy-cluster interactions from the point of view of the actor, or either gravitational (mass-mass) or hy-

drodynamic (gas-gas) interactions in terms of physical process. Figure 12 suggests that the galaxy-cluster tidal interactions are responsible for structural and kinematic changes of cluster late-type galaxies toward early morphological type. Late types seem to become more spheroidal through such interactions. Figure 10 indicates that the hydrodynamic interactions with early-type neighbors are responsible for reddening and SFA quenching of cluster late-type galaxies. Therefore, the morphology transformation of late-type galaxies seems to take place in clusters through galaxy-galaxy hydrodynamic interactions and galaxy-cluster/galaxy-galaxy gravitational interactions. However, it is reasonable to accept that all above mechanisms are contributing to the MRR/MDR in clusters to some extent and a particular process cannot fully account for all observational aspects.

5. CONCLUSIONS

We have studied the dependence of various galaxy properties on the clustercentric radius and the environment attributed to the nearest neighbor galaxy using the SDSS galaxies associated with the Abell galaxy clusters. Our major findings are as follows.

1. There exists a characteristic scale where the galaxy properties such as morphology, color gradient, and structural parameters suddenly start to depend on the clustercentric radius at fixed nearest neighbor environment.

2. The characteristic scale depends on galaxy luminosity; the faint galaxies with $-17.0 \geq M_r > -19.0$ has the scale at $\sim 3r_{200,\mathrm{cl}}$ while the scale is $\sim r_{200,\mathrm{cl}}$ for the brighter galaxies with $-20.5 \geq M_r > -22.5$.

3. The hydrodynamic interactions with nearby early-type galaxies seem to be the main drive to quenching star formation activity of late-type galaxies in clusters. We do not find evidence that the hot cluster gas is the main drive down to the clustercentric radius of $\sim 0.1r_{200,\mathrm{cl}}$.

4. The interaction with the cluster potential and harassment are the viable mechanisms that can account for the clustercentric radius dependence of the structural and internal kinematics parameters.

Existence of the characteristic scale means that the local galaxy number density is not responsible for the MDR in cluster because the local density is a smooth function of the clustercentric radius and has no discontinuity in general. The MDR appears working in clusters and also in the field because of the statistical correlation between the local density and the nearest neighbor distance. What is really working in clusters is the morphology-clustercentric radius-neighbor environment relation, where the neighbor environment means both neighbor morphology and the mass density attributed to the neighbor.

According to the third and fourth conclusions, the morphology transformation of the late-type galaxies in clusters is not due to a single mechanism and has been taken place through both hydrodynamic and gravitational processes.

We would like to thank the anonymous referee for useful comments. The authors acknowledge the support of the Korea Science and Engineering Foundation (KOSEF) through the Astrophysical Research Center for the Structure and Evolution of the Cosmos (ARCSEC).

Funding for the SDSS and SDSS-II has been provided by the Alfred P. Sloan Foundation, the Participating Institutions, the National Science Foundation, the U.S. Department of Energy, the National Aeronautics and Space Administration, the Japanese Monbukagakusho, the Max Planck Society, and the Higher Education Funding Council for England. The SDSS Web Site is http://www.sdss.org/.

The SDSS is managed by the Astrophysical Research Consortium for the Participating Institutions. The Participating Institutions are the American Museum of Natural History, Astrophysical Institute Potsdam, University of Basel, Cambridge University, Case Western Reserve University, University of Chicago, Drexel University, Fermilab, the Institute for Advanced Study, the Japan Participation Group, Johns Hopkins University, the Joint Institute for Nuclear Astrophysics, the Kavli Institute for Particle Astrophysics and Cosmology, the Korean Scientist Group, the Chinese Academy of Sciences (LAMOST), Los Alamos National Laboratory, the Max-Planck-Institute for Astronomy (MPIA), the Max-Planck-Institute for Astrophysics (MPA), New Mexico State University, Ohio State University, University of Pittsburgh, University of Portsmouth, Princeton University, the United States Naval Observatory, and the University of Washington.

This research has made use of the NASA/IPAC Extragalactic Database (NED) which is operated by the Jet Propulsion Laboratory, California Institute of Technology, under contract with the National Aeronautics and Space Administration.

APPENDIX

We calculate the cluster velocity dispersion by using the cluster member galaxies after excluding the interlopers. To find the interlopers among the cluster galaxies, we compute δ for each galaxy, which indicates the local deviations from the systemic velocity (v_{sys}) and dispersion ($\sigma_{\mathrm{cl,all}}$) of the entire cluster (Dressler & Shectman 1988). It is defined by

$$\delta^2 = \frac{N_{nn}}{\sigma^2_{\mathrm{cl,all}}} \left[(v_{\mathrm{local}} - v_{\mathrm{sys}})^2 + (\sigma_{\mathrm{local}} - \sigma_{\mathrm{cl,all}})^2 \right], \quad (1)$$

where N_{nn} is the number of the nearest galaxies that defines the local environment, taken to be ${N_{\mathrm{gal}}}^{1/2}$ in this study. N_{gal} is the total number of member galaxies in the cluster. The nearest galaxies are those located closest to the galaxy on the sky. v_{local} and σ_{local} are systematic velocity and its dispersion estimated from N_{nn} nearest galaxies, respectively. We use the galaxies with $\delta \leq 3.0$ to compute the cluster velocity dispersion.

REFERENCES

Abell G. O., Corwin H. G., & Olowin R. P., 1989, ApJS, 70, 1

Adelman-McCarthy, J. K., et al. 2008, ApJS, 175, 297

Ann, H. B., Park, C., & Choi, Y.-Y. 2008, MNRAS, 389, 86
Bekki, K., Couch, W. J., & Shioya, Y. 2002, ApJ, 577, 651
Blanton, M. R., Lin, H., Lupton, R. H., Maley, F. M., Young, N., Zehavi, I., & Loveday, J. 2003, AJ, 125, 2276
Blanton, M. R., Eisenstein, D., Hogg, D. W., Schlegel, D. J., & Brinkmann, J. 2005, AJ, 129, 2562
Böhringer, H., et al. 2000, ApJS, 129, 435
Böhringer, H., et al. 2004, A&A, 425, 367
Boselli, A., & Gavazzi, G. 2006, PASP, 118, 517
Bruzual, G., & Charlot, S. 2003, MNRAS, 344, 1000
Byrd, G., & Valtonen, M. 1990, ApJ, 350, 89
Carlberg, R. G., Yee, H. K. C., & Ellingson, E. 1997, ApJ, 478, 462
Castander, F. J., et al. 2001, AJ, 121, 2331
Choi, Y.-Y., Park, C., & Vogeley, M. S. 2007, ApJ, 658, 884
Cowie, L. L., & Songaila, A. 1977, Nature, 266, 501
Christlein, D., & Zabludoff, A. I. 2005, ApJ, 621, 201
Domínguez, M., Muriel, H., & Lambas, D. G. 2001, AJ, 121, 1266
Dressler, A. 1980, ApJ, 236, 351
Dressler A., & Shectman S. A., 1988, AJ, 95, 985
Dressler, A., et al. 1997, ApJ, 490, 577
Fadda D., Girardi M., Giuricin G., Mardirossian F., & Mezzetti M., ApJ, 473, 670
Farouki, R., & Shapiro, S. L. 1981, ApJ, 243, 32
Fukugita, M., Ichikawa, T., Gunn, J. E., Doi, M., Shimasaku, K., & Schneider, D. P. 1996, AJ, 111, 1748
Gnedin, O. Y. 2003, ApJ, 589, 752
Goto, T., Yamauchi, C., Fujita, Y., Okamura, S., Sekiguchi, M., Smail, I., Bernardi, M., & Gomez, P. L. 2003, MNRAS, 346, 601
Gott, J. R., & Rees, M. J. 1975, A&A, 45, 365
Gunn, J. E., & Gott, J. R. 1972, ApJ, 176, 1
Gunn, J. E., et al. 1998, AJ, 116, 3040
Gunn, J. E., et al. 2006, AJ, 131, 2332
Hogg, D. W., Finkbeiner, D. P., Schlegel, D. J., & Gunn, J. E. 2001, AJ, 122, 2129
Hwang, H. S., & Lee, M. G. 2007, ApJ, 662, 236
Hwang, H. S., & Lee, M. G. 2008, ApJ, 676, 218
Hwang, H. S., & Park, C. 2008, ApJ, submitted
Hubble, E., & Humason, M. L. 1931, ApJ, 74, 43
Icke, V. 1985, A&A, 144, 115
Ivezić, Ž., et al. 2004, Astronomische Nachrichten, 325, 583
Larson, R. B., Tinsley, B. M., & Caldwell, C. N. 1980, ApJ, 237, 692
Lupton, R. H., Ivezic, Z., Gunn, J. E., Knapp, G., Strauss, M. A., & Yasuda, N. 2002, Proc. SPIE, 4836, 350
Merritt, D. 1983, ApJ, 264, 24
Merritt, D. 1984, ApJ, 276, 26
Miller, R. H. 1986, A&A, 167, 41
Moore, B., Katz, N., Lake, G., Dressler, A., & Oemler, A. 1996, Nature, 379, 613
Moore, B., Lake, G., & Katz, N. 1998, ApJ, 495, 139
Moore, B., Lake, G., Quinn, T., & Stadel, J. 1999, MNRAS, 304, 465
Moss, C., & Whittle, M. 2000, MNRAS, 317, 667
Nulsen, P. E. J. 1982, MNRAS, 198, 1007
Park, C., & Choi, Y.-Y. 2005, ApJ, 635, L29
Park, C., & Choi, Y.-Y. 2009, ApJ, 691, 1828
Park, C., Choi, Y.-Y., Vogeley, M. S., Gott, J. R., & Blanton, M. R. 2007, ApJ, 658, 898
Park, C., Gott, J. R., & Choi, Y.-Y. 2008, ApJ, 674, 784
Peebles, P. J. E. 1993, Princeton Series in Physics, Princeton, NJ: Princeton University Press
Pier, J. R., Munn, J. A., Hindsley, R. B., Hennessy, G. S., Kent, S. M., Lupton, R. H., & Ivezić, Ž. 2003, AJ, 125, 1559
Poggianti, B. M., et al. 2008, ApJ, 684, 888
Postman, M., et al. 2005, ApJ, 623, 721
Quilis, V., Moore, B., & Bower, R. 2000, Science, 288, 1617
Quintero, A. D., Berlind, A. A., Blanton, M., & Hogg, D. W. 2006, ApJ, submitted (astro-ph/0611361)
Richstone, D. O. 1976, ApJ, 204, 642
Schlegel, D. J., Finkbeiner, D. P., & Davis, M. 1998, ApJ, 500, 525
Skibba R. A., et al. 2008, MNRAS, submitted (astro-ph/0811.3970)
Smith, J. A., et al. 2002, AJ, 123, 2121
Smith, G. P., Treu, T., Ellis, R. S., Moran, S. M., & Dressler, A. 2005, ApJ, 620, 78
Spitzer, L. J., & Baade, W. 1951, ApJ, 113, 413
Stoughton, C., et al. 2002, AJ, 123, 485
Tegmark, M., et al. 2004, ApJ, 606, 702
Thomas, T., & Katgert, P. 2006, A&A, 446, 31
Tremonti, C. A., et al. 2004, ApJ, 613, 898
Treu, T., Ellis, R. S., Kneib, J.-P., Dressler, A., Smail, I., Czoske, O., Oemler, A., & Natarajan, P. 2003, ApJ, 591, 53
Tucker, D. L., et al. 2006, Astronomische Nachrichten, 327, 821
Uomoto, A., et al. 1999, Bulletin of the American Astronomical Society, 31, 1501
Weinmann, S. M., van den Bosch, F. C., Yang, X., & Mo, H. J. 2006, MNRAS, 366, 2
Whitmore, B. C., Gilmore, D. M., & Jones, C. 1993, ApJ, 407, 489
York, D. G., et al. 2000, AJ, 120, 1579